

# Electroweak precision tests of composite Higgs models

---

Mads T. Frandsen<sup>a</sup> and Martin Rosenlyst<sup>b</sup>

<sup>a</sup>*CP<sup>3</sup>-Origins, University of Southern Denmark, Campusvej 55, DK-5230 Odense M, Denmark*

<sup>b</sup>*Rudolf Peierls Centre for Theoretical Physics, University of Oxford, 1 Keble Road, Oxford OX1 3NP, United Kingdom*

*E-mail:* [frandsen@cp3.sdu.dk](mailto:frandsen@cp3.sdu.dk), [martin.jorgensen@physics.ox.ac.uk](mailto:martin.jorgensen@physics.ox.ac.uk)

**ABSTRACT:** We study constraints on Composite Higgs models with fermion partial compositeness from electroweak precision measurements, including the 2022  $W$ -boson mass result from the CDF collaboration. We focus on models where the Composite Higgs sector arises from underlying four-dimensional strongly interacting gauge theories with fermions, and where the SM fermions obtain their mass via linear mixing terms between the fermions and the composite sector — the so-called fermion partial compositeness scenario. In general, the Composite Higgs sector leads to a small and positive  $S$  parameter, and a negative  $T$  parameter, but the fermion partial compositeness sector results in an overall positive  $T$  parameter in a large part of parameter space. We, therefore, find good agreement between the full composite models and the current electroweak precision measurement bounds on  $S$  and  $T$  from LEP and CDF, including the offset and correlation of  $S, T$  with respect to the SM predictions.

---

## Contents

<b>1</b>	<b>Introduction</b>	<b>1</b>
<b>2</b>	<b>A minimal composite Higgs model</b>	<b>3</b>
2.1	The underlying Lagrangian	3
2.2	The effective Lagrangian	4
<b>3</b>	<b>The effective theory of the spin-1 resonances</b>	<b>6</b>
<b>4</b>	<b>The effective theory of the fermion resonances</b>	<b>8</b>
<b>5</b>	<b>The effective potential and vacuum misalignment</b>	<b>11</b>
<b>6</b>	<b>Contributions to the oblique parameters</b>	<b>12</b>
6.1	Modification of the Higgs couplings	12
6.2	The composite spin-1 resonances	13
6.3	The fermion resonances	13
<b>7</b>	<b>Generalization to other 4D CH models</b>	<b>17</b>
<b>8</b>	<b>CH models with coset <math>\text{SO}(N_f)/\text{SO}(N_f - 1)</math></b>	<b>18</b>
<b>9</b>	<b>Conclusions</b>	<b>19</b>

---

## 1 Introduction

The fundamental origin of the Higgs sector of the Standard Model (SM) and the related naturalness and triviality problems are important problems in particle physics. A dynamical origin of the Higgs sector and electroweak symmetry breaking (EWSB) is an appealing possible solution of these problems. In “Composite Higgs” (CH) models [1, 2], the Higgs boson arises as a composite pseudo-Nambu-Goldstone boson (pNGB) from a spontaneously broken global symmetry.<sup>1</sup> It can therefore be naturally light with respect to the compositeness scale and other composite resonances in the model — in agreement with current observations.

In this paper, we will further assume the global symmetry arises from the chiral symmetries of fermions of an underlying confining gauge-fermion theory. The interactions between the SM sector and the new composite sector breaks the global symmetry group  $G$  explicitly and triggers dynamical EWSB yielding masses for the SM electroweak gauge

---

<sup>1</sup>In general, composite Higgs models were first proposed in Refs. [3, 4], but in these models the Higgs boson is not identified as a light pNGB candidate.

bosons. We also assume that the SM fermions gain their masses through a linear mixing of the SM fermions with composite fermions of the new strongly interacting sector, the so-called fermion ‘‘Partial Compositeness’’ (PC) mechanism [5]. Generating the SM fermion masses, including the heavy top quark mass, without violating flavour changing neutral current (FCNCs) constraints is a well-known challenge in composite models [6]. The PC mechanism provides a possibility to achieve this provided the composite fermionic operators that linearly coupled to the top quark have sufficiently large anomalous dimensions. The PC operators also contribute to the so-called oblique electroweak parameters  $S$ ,  $T$  and  $U$  [7, 8], in particular to the  $T$  parameter. In Ref. [9], it is e.g. shown that the PC sector in the  $SO(5)/SO(4)$  CH model may contribute positively to the  $T$  parameter, which is also reviewed in details in Ref. [10]. On the other hand, the composite Higgs sector itself contributes to a positive  $S$  parameter.

The contributions to the  $S$  and  $T$  parameters from CH models can be tested by the precise measurements of electroweak precision observables performed at LEP [11], Tevatron [12] and LHC [13]. Recently, the CDF collaboration published an updated more precise measurement of the  $W$  boson mass,  $m_W^{\text{CDF}} = 80,433.5 \pm 9.4$  MeV [12], that differs with  $7\sigma$  significance from the SM prediction,  $m_W^{\text{SM}} = 80,357 \pm 6$  MeV [14], and also from the LEP,  $D\bar{O}$ , CDF and ATLAS measurements:  $m_W^{\text{LEP}} = 80,385 \pm 15$  MeV from LEP [15] and  $m_W^{\text{ATLAS}} = 80,370 \pm 19$  MeV from ATLAS [13].

By assuming  $U = 0$ , the recent CDF measurement of the  $W$  mass can be translated to best fit values for the  $S$  and  $T$  parameters [16, 17]:

$$S = 0.06 \pm 0.08, \quad T = 0.15 \pm 0.06 \quad (1.1)$$

with a strong correlation  $\rho \approx 0.95$ . while the previous Particle Data Group (PDG) value before the CDF measurement was [14]

$$S = 0.00 \pm 0.07, \quad T = 0.05 \pm 0.06 \quad (1.2)$$

with the correlation  $\rho \approx 0.92$ .

In this paper, we explore the parameter space of Composite Higgs models in light of these electroweak precision constraints. In particular, we show that the observed offset and correlation of  $S$  and  $T$ , with respect to the SM prediction, arises in a large part of the explored parameter space. I.e. in a large part of the viable parameter space, we find a positive contribution to the  $S$  parameter from the composite higgs sector and a positive contribution to  $T$  from the fermion PC sector — in agreement with the combined LEP and CDF precision measurements.<sup>2</sup>

We focus on a minimal CH model realization with  $G/H = SU(4)/Sp(4) \sim SO(6)/SO(5)$  [19] as template<sup>3</sup>, and provide a discussion of how our results generalize to non-minimal CH models. In the CH framework with extended global symmetries, the dark matter may

---

<sup>2</sup>In Ref. [18], it is shown that this agreement is also naturally accommodated in other dynamical models such as the dilaton Higgs, the Technicolor and glueball Higgs.

<sup>3</sup>The smaller  $SO(5) \rightarrow SO(4)$  coset is difficult to realize in a simple manner from a 4D gauge-fermion theory but arises more simply in the 5D holographic approach [20].

	$G_{\text{HC}}$	$SU(2)_W$	$U(1)_Y$
$(U_L, D_L)$	$\square$	$\square$	0
$\tilde{U}_L$	$\square$	1	-1/2
$\tilde{D}_L$	$\square$	1	+1/2

**Table 1.** The new fermion content and their representations under the gauge groups.

be predicted as composite pNGB candidates, typically producing thermal DM [23–27] and in some models non-thermal candidates [28–31]. These models may be tested by the results in this paper. Furthermore, if the 2022 CDF results are interpreted in terms of Composite Higgs models they may offer a striking first window into origin of the SM fermion masses. It will be very interesting to further explore the implications for distinguishing between different possible fermion mass origins, in particular “Extended Technicolor” (ETC) [21] and the complementarity with other probes of these mass origins [22].

## 2 A minimal composite Higgs model

The possible chiral symmetry breaking patterns in CH models based on an underlying four-dimensional gauge theory of strongly interacting fermions (hyper-fermions) are discussed in Refs. [32, 33]. Given  $N_f$  Weyl spinors transforming in the representation  $\mathcal{R}$  of the confining hypercolor (HC) group  $G_{\text{HC}}$ , the three possible vacuum cosets upon chiral symmetry breaking are [34]:  $SU(N_f)/SO(N_f)$  for real  $\mathcal{R}$ ,  $SU(N_f)/\text{Sp}(N_f)$  for pseudo-real  $\mathcal{R}$  and  $SU(N_f) \otimes SU(N_f) \otimes U(1)/SU(N_f) \otimes U(1)$  for complex  $\mathcal{R}$ . The minimal CH cosets for these three types contain  $N = 5$  in the real case [2],  $N = 4$  in both the pseudo-real [19] and the complex cases [23]. In terms of pNGB spectrum, the pseudo-real case is the most minimal with only five composite pNGB states. Therefore, we consider concretely the minimal coset  $SU(4)/\text{Sp}(4)$  [19] providing both a Higgs candidate and custodial symmetry, where hyper-fermions and their representations under the electroweak gauge group and the HC gauge group  $G_{\text{HC}}$  are listed in Table 1.

### 2.1 The underlying Lagrangian

This minimal symmetry breaking pattern  $SU(4) \rightarrow \text{Sp}(4)$  can thus be achieved if the hyper-fermions are in a pseudo-real representation of the HC gauge group: this can be minimally achieved for  $G_{\text{HC}} = SU(2)_{\text{HC}}$  or  $\text{Sp}(2N)_{\text{HC}}$  (or  $SO(N)_{\text{HC}}$ ) with the hyper-fermions in the fundamental (or spin) representation. The four Weyl hyper-fermions can be arranged into an  $SU(4)_Q$  vector  $Q \equiv (U_L, D_L, \tilde{U}_L, \tilde{D}_L)^T$ . In terms of this fourplet, the underlying gauge-fermion Lagrangian of the CH model can be written as

$$\mathcal{L}_{\text{CH}} = Q^\dagger i\gamma^\mu D_\mu Q - \frac{1}{2} (Q^T M_Q Q + \text{h.c.}) + \mathcal{L}_{\text{PC}}, \quad (2.1)$$

where the covariant derivative include the HC-gluons and the  $SU(2)_L$  and  $U(1)_Y$  gauge bosons. The mass term contributes to the correct vacuum alignment in between the EW

unbroken vacuum and a Technicolor vacuum, and consists of two independent masses  $\bar{m}_{1,2}$  for the doublet and singlet hyper-fermions,  $M_Q = \text{Diag}(i\bar{m}_1\sigma_2, -i\bar{m}_2\sigma_2)$ , where  $\sigma_2$  is the second Pauli matrix.

The terms in  $\mathcal{L}_{\text{PC}}$  in Eq. (2.1) are interactions responsible for generating the masses and Composite Higgs-Yukawa couplings for the SM fermions in the condensed phase. The PC operators of  $\mathcal{L}_{\text{PC}}$  require the extension of the model in Table 1 by a new species of fermions  $\chi_t$ , transforming under the two-index anti-symmetric representation of  $G_{\text{HC}} = \text{Sp}(2N)_{\text{HC}}$ , and carrying appropriate quantum numbers under the SM gauge symmetry. For the top, it is enough to introduce a  $\text{SU}(2)_W$  vector-like pair with hypercharge  $+2/3$  and transforming as a fundamental of the ordinary  $\text{SU}(3)_C$  color gauge group (QCD). Models of this type were first proposed in Refs. [35, 36] and our model is an extension of the one in Ref. [35].

We arrange the new QCD colored hyper-fermions into an  $\text{SU}(6)_\chi$  vector, which will spontaneously break to  $\text{SO}(6)_\chi$  upon the condensation. Thus, we study the minimal CH model with global symmetry breaking pattern

$$\frac{\text{SU}(4)_Q}{\text{Sp}(4)_Q} \otimes \frac{\text{SU}(6)_\chi}{\text{SO}(6)_\chi} \otimes \frac{\text{U}(1)_Q \otimes \text{U}(1)_\chi}{\emptyset}, \quad (2.2)$$

where one of the subgroups of  $\text{U}(1)_Q \otimes \text{U}(1)_\chi$  has an anomaly with the hypercolor symmetry group,  $G_{\text{HC}}$ , while the other one is an anomaly-free subgroup  $\text{U}(1)_\sigma$ . Moreover, the QCD gauge group  $\text{SU}(3)_C$  will be identified as a subgroup of the unbroken group  $\text{SO}(6)_\chi$ . This global symmetry breaking pattern can thus determine the possible hypercolor groups [36], which can only be  $G_{\text{HC}} = \text{Sp}(2N)_{\text{HC}}$  with  $2 \leq N \leq 18$  (or  $G_{\text{HC}} = \text{SO}(N)_{\text{HC}}$  with  $N = 11, 13$  for  $Q$  and  $\chi$  transforming, respectively, in the spin and fundamental representations under  $G_{\text{HC}}$ ). Therefore, the minimal choice is  $G_{\text{HC}} = \text{Sp}(4)_{\text{HC}}$ .

The four-fermion interactions that will generate the PC operators we consider are [37]:

$$\frac{\tilde{y}_L}{\Lambda_t^2} q_{L,3}^{\alpha\dagger} (Q^\dagger P_q^\alpha Q^* \chi_t^\dagger) + \frac{\tilde{y}_R}{\Lambda_t^2} t_R^{c\dagger} (Q^\dagger P_t Q^* \chi_t^\dagger) + \text{h.c.}, \quad (2.3)$$

where  $q_{L,3}$  and  $t_R$  are the third generation of the quark doublets and the top singlet, respectively, and  $P_q$  and  $P_t$  are spurions that project onto the appropriate components in the fourplet  $Q$ . For both the left- and right-handed top, we choose the spurions to transform as the two-index anti-symmetric of the unbroken chiral symmetry subgroup  $\text{SU}(4)_Q$  as the minimal possible choice. Concretely, the spurions are given in matrix form in Ref. [37].

## 2.2 The effective Lagrangian

Upon the condensation of the hyper-fermions at a scale  $\Lambda_{\text{HC}} \sim 4\pi f$ , where  $f$  is the decay constant of the composite pNGBs they can form an anti-symmetric and SM gauge invariant condensate of the form

$$\langle Q_{\alpha,a}^I Q_{\beta,b}^J \rangle \epsilon^{\alpha\beta} \epsilon^{ab} \sim \Sigma_{Q0}^{IJ} = \begin{pmatrix} i\sigma_2 & 0 \\ 0 & -i\sigma_2 \end{pmatrix}, \quad (2.4)$$

where  $\alpha, \beta$  are spinor indices,  $a, b$  are HC indices, and  $I, J$  are flavour indices of the hyper-fermions. This condensate visibly breaks  $\text{SU}(4)_Q \rightarrow \text{Sp}(4)_Q$  via an anti-symmetric tensor [19], resulting in five pNGBs,  $\pi_A$  with  $A = 1, \dots, 5$ , corresponding to the broken

generators,  $X_A$ , and ten unbroken generators  $T_{\bar{A}}$  with  $\bar{A} = 1, \dots, 10$ . Here the unbroken generators  $T_{\bar{A}} = \{T_L^a, T_R^a, T_r^i\}$  with  $a = 1, 2, 3$  and  $i = 1, \dots, 4$ , in which  $T_{L,R}^a$  belong to the custodial symmetry subgroup  $\text{SO}(4)_C \cong \text{SU}(2)_L \otimes \text{SU}(2)_R$  while  $T_r^i$  belong to the coset  $\text{Sp}(4)_Q/\text{SO}(4)_C$ . In the following, we identify  $T_L^a$  and  $T_R^3$  as the generators for the  $\text{SU}(2)_L$  and  $\text{U}(1)_Y$  gauge groups, respectively. The explicit matrix form of all these generators are listed in Ref. [19].

We parameterize the pNGBs as  $U_Q = \exp[i\pi_A X_A/f]$ , where  $f$  is their decay constant. In the following, we identify the composite pNGB Higgs candidate as  $h \equiv \pi_4$  and a pseudo-scalar  $\eta \equiv \pi_5$ , while the additional three are the Goldstones eaten by the  $W^\pm$  and  $Z$  gauge bosons. In the unitary gauge, we can write

$$U_Q = \begin{pmatrix} (c_Q + i\frac{\eta}{\pi_Q} s_Q) \mathbf{1}_2 & i\sigma_2 \frac{h}{\pi_Q} s_Q \\ i\sigma_2 \frac{h}{\pi_Q} s_Q & (c_Q - i\frac{\eta}{\pi_Q} s_Q) \mathbf{1}_2 \end{pmatrix}, \quad (2.5)$$

where  $c_Q \equiv \cos(\pi_Q/(2f))$  and  $s_Q \equiv \sin(\pi_Q/(2f))$  with  $\pi_Q \equiv \sqrt{h^2 + \eta^2}$ . Finally, the explicit form of the pNGB matrix with coset  $\text{SU}(4)_Q/\text{Sp}(4)_Q$  is given by  $\Sigma_Q = U_Q^2 \Sigma_{Q0}$ .

Below the compositeness scale  $\Lambda_{\text{HC}}$ , Eq. (2.1) is replaced by the effective Lagrangian:

$$\mathcal{L}_{\text{eff}} = \mathcal{L}_{\text{kin}} - V_{\text{eff}}. \quad (2.6)$$

Here  $\mathcal{L}_{\text{kin}}$  is the usual leading order ( $\mathcal{O}(p^2)$ ) chiral Lagrangian [6],

$$\mathcal{L}_{\text{kin}, p^2} = \frac{f^2}{4} \text{Tr}[d_\mu d^\mu], \quad (2.7)$$

where the  $d$  and  $e$  symbols of this model are given by the Maurer-Cartan form

$$iU_Q^\dagger D_\mu U_Q \equiv d_\mu^A X^A + e_\mu^{\bar{A}} T^{\bar{A}} \equiv d_\mu + e_\mu, \quad (2.8)$$

with the gauge covariant derivative

$$D_\mu = \partial_\mu - igW_\mu^a T_L^a - ig'B_\mu T_R^3. \quad (2.9)$$

Besides providing kinetic terms in Eq. (2.7) and self-interactions for the pNGBs, it will induce masses for the EW gauge bosons and their couplings with the pNGBs (including the SM Higgs identified as  $h$ ),

$$\begin{aligned} m_W^2 &= \frac{1}{4} g^2 f^2 \sin^2 \left( \frac{\langle h \rangle}{f} \right), & m_Z^2 &= m_W^2 / c_{\theta_W}^2, \\ g_{hWW} &= \frac{1}{4} g^2 f \sin \left( \frac{2\langle h \rangle}{f} \right) = g_{hWW}^{\text{SM}} \cos \left( \frac{\langle h \rangle}{f} \right), & g_{hZZ} &= g_{hWW} / c_{\theta_W}^2, \end{aligned} \quad (2.10)$$

where  $\theta_W$  is the Weinberg angle,  $g$  is the weak  $\text{SU}(2)_L$  gauge coupling and

$$\sin \theta \equiv \sin \left( \frac{\langle h \rangle}{f} \right) \equiv \frac{v_{\text{SM}}}{f}, \quad v_{\text{SM}} = 246 \text{ GeV}. \quad (2.11)$$

The vacuum misalignment angle  $\theta$  parametrizes the deviations of the CH Higgs couplings to the EW gauge bosons with respect to the SM Higgs. These deviations are constrained

by direct LHC measurements [38] of this coupling which imply an upper bound of  $s_\theta \lesssim 0.3$ . EW precision measurements also impose an upper limit which has been found to be stricter  $s_\theta \lesssim 0.2$  [6]. However, in this study, we find that the constraints on  $s_\theta$  from EW precision measurements are alleviated when we include all contributions from the composite fermion resonances in the CH models

In Section 5, we write the effective potential  $V_{\text{eff}}$  in Eq. (2.6) to leading order, which receives contributions from the hyper-fermion masses  $\overline{m}_{1,2}$  in Eq. (2.1), and from integrating out the composite fermion, vector and axial-vector resonances in the effective theory. By minimizing this effective potential  $V_{\text{eff}}$ , the misalignment angle  $\theta$  can be determined. The physics of these composite resonances are discussed in the following two sections.

### 3 The effective theory of the spin-1 resonances

The composite spin-1 resonances, analogous to the  $\rho$ - and  $a_1$ -mesons in the QCD can be organized into a **10**-plet  $V_\mu = V_\mu^{\bar{A}} T^{\bar{A}}$  of the unbroken  $\text{Sp}(4)_Q$  and a **5**-plet  $A_\mu = A_\mu^A X^A$  in  $\text{SU}(4)_Q/\text{Sp}(4)_Q$  with  $\bar{A} = 1, \dots, 10$  and  $A = 1, \dots, 5$ . Here  $T^{\bar{A}}$  and  $X^A$  are, respectively, the ten unbroken generators of  $\text{Sp}(4)_Q$  and the five broken generators in  $\text{SU}(4)_Q/\text{Sp}(4)_Q$ . Under the decomposition  $\text{Sp}(4)_Q \rightarrow \text{SU}(2)_L \otimes \text{U}(1)_Y$ , these objects decompose into

$$\left( \begin{array}{l} \mathbf{10} \rightarrow \mathbf{3}_0 \oplus \mathbf{1}_1 \oplus \mathbf{1}_0 \oplus \mathbf{1}_{-1} \oplus \mathbf{2}_{1/2} \oplus \mathbf{2}_{-1/2} \\ V \rightarrow V_L \oplus V_R^+ \oplus V_R^0 \oplus V_R^- \oplus V_D \oplus \tilde{V}_D \end{array} \right), \quad \left( \begin{array}{l} \mathbf{5} \rightarrow \mathbf{2}_{1/2} \oplus \mathbf{2}_{-1/2} \oplus \mathbf{1}_0 \\ A \rightarrow A_D \oplus \tilde{A}_D \oplus A_S \end{array} \right), \quad (3.1)$$

where  $\tilde{V}_D = i\sigma_2 V_D^*$  and  $\tilde{A}_D = i\sigma_2 A_D^*$ .

In the following, we will use the hidden gauge symmetry formalism to describe the spin-1 resonances, as done in Ref. [39]. We therefore formally extend the global symmetry group  $\text{SU}(4)_Q$  to  $\text{SU}(4)_1 \otimes \text{SU}(4)_2$ . We embed the elementary SM gauge bosons in  $\text{SU}(4)_1$  and the heavy composite spin-1 resonances in  $\text{SU}(4)_2$ . In the effective Lagrangian, the  $\text{SU}(4)_i$  ( $i = 1, 2$ ) symmetries are spontaneously broken to  $\text{Sp}(4)_i$  via the introduction of two nonlinear representations  $U_i$  containing five pNGBs each (similar to the pNGB matrix  $U_Q$  in Eq. (2.5)), which are given by

$$U_1 = \exp \left( \frac{i}{f_1} \sum_{A=1}^5 \pi_1^A X^A \right), \quad U_2 = \exp \left( \frac{i}{f_2} \sum_{A=1}^5 \pi_2^A X^A \right). \quad (3.2)$$

They transform as  $U_i \rightarrow g_i U_i h(g_i, \pi_i)^\dagger$ , where  $g_i$  and  $h(g_i, \pi_i)$  are group elements of  $\text{SU}(4)_i$  and  $\text{Sp}(4)_i$ , respectively. Furthermore, the breaking of  $\text{Sp}(4)_1 \otimes \text{Sp}(4)_2$  into the chiral subgroup  $\text{Sp}(4)_Q$  is described by the field

$$K = \exp \left( \frac{i}{f_K} \sum_{\bar{A}=1}^{10} k^{\bar{A}} T^{\bar{A}} \right), \quad (3.3)$$

containing ten pNGBs corresponding to the generators of  $\text{Sp}(4)$  and transforming like  $K \rightarrow h(g_1, \pi_1) K h(g_2, \pi_2)^\dagger$ .

To write down the effective Lagrangian for the spin-1 resonances and  $K$ , we define the gauged Maurer-Cartan one-forms as

$$\begin{aligned}\Omega_{i,\mu} &\equiv iU_i^\dagger D_\mu U_i \\ &\equiv d_{i,\mu}^A X^A + e_{i,\mu}^{\bar{A}} T^{\bar{A}} \equiv d_{i,\mu} + e_{i,\mu},\end{aligned}\quad (3.4)$$

where the covariant derivatives are given by

$$\begin{aligned}D_\mu U_1 &= (\partial_\mu - igW_\mu^a T_L^a - ig' B_\mu T_R^3) U_1, \\ D_\mu U_2 &= (\partial_\mu - i\tilde{g}V_\mu^{\bar{A}} T^{\bar{A}} - i\tilde{g}A_\mu^A X^A) U_2,\end{aligned}\quad (3.5)$$

such that the heavy spin-1 vectors are formally introduced like gauge fields similarly to the SM gauge fields. The covariant derivative of  $K$  has the form

$$D_\mu K = \partial_\mu K - ie_{1,\mu} K + iK e_{2,\mu}. \quad (3.6)$$

Here the  $d$  and  $e$  symbols transform under  $SU(4)_i$  as follows

$$d_{i,\mu} \rightarrow h(g_i, \pi_i) d_{i,\mu} h(g_i, \pi_i)^\dagger, \quad e_{i,\mu} \rightarrow h(g_i, \pi_i) (e_{i,\mu} + i\partial_\mu) h(g_i, \pi_i)^\dagger. \quad (3.7)$$

Thus, the effective Lagrangian of the spin-1 resonances is given by

$$\begin{aligned}\mathcal{L}_{\text{gauge}} &= -\frac{1}{2g^2} \text{Tr}[W_{\mu\nu} W^{\mu\nu}] - \frac{1}{2g'^2} \text{Tr}[B_{\mu\nu} B^{\mu\nu}] - \frac{1}{2\tilde{g}} \text{Tr}[V_{\mu\nu} V^{\mu\nu}] - \frac{1}{2\tilde{g}} \text{Tr}[A_{\mu\nu} A^{\mu\nu}] \\ &+ \frac{1}{2} f_1^2 \text{Tr}[d_{1,\mu} d_1^\mu] + \frac{1}{2} f_2^2 \text{Tr}[d_{2,\mu} d_2^\mu] + r f_2^2 \text{Tr}[d_{1,\mu} K d_2^\mu K^\dagger] + \frac{1}{2} f_K^2 \text{Tr}[D_\mu K D^\mu K^\dagger],\end{aligned}\quad (3.8)$$

where

$$\begin{aligned}W_{\mu\nu} &= \partial_\mu W_\nu - \partial_\nu W_\mu - ig[W_\mu, W_\nu], & B_{\mu\nu} &= \partial_\mu B_\nu - \partial_\nu B_\mu, \\ V_{\mu\nu} &= \partial_\mu V_\nu - \partial_\nu V_\mu - i\tilde{g}[V_\mu, V_\nu], & A_{\mu\nu} &= \partial_\mu A_\nu - \partial_\nu A_\mu - i\tilde{g}[A_\mu, A_\nu]\end{aligned}\quad (3.9)$$

with  $W_\mu = W_\mu^a T_L^a$ . We have omitted terms containing a scalar singlet  $\sigma$  resonance, included in Ref. [39], as we here assume this resonance is heavy.

In terms of the above Lagrangian parameters, we define the mass parameters

$$m_V \equiv \frac{\tilde{g} f_K}{\sqrt{2}}, \quad m_A \equiv \frac{\tilde{g} f_1}{\sqrt{2}}. \quad (3.10)$$

The masses of  $V_D$  and  $\tilde{V}_D$  are  $m_V$ , while the masses of  $A_S$  and the axial combination of  $A_D$  and  $\tilde{A}_D$  are  $m_A$  as these vector resonances, given in Eq. (3.1), do not mix with the SM vector states. The explicit mass expressions of the additional gauge bosons are given in Ref. [39].

After integrating out the heavy resonances in Eq. (3.8), we obtain under the unitary gauge the Lagrangian

$$\begin{aligned}\mathcal{L}_{\text{eff}}^{\text{gauge}} &= \frac{1}{2} P_T^{\mu\nu} \left[ \left( -p^2 + \frac{g'^2}{g^2} \Pi_0(p) \right) B_\mu B_\nu + (-p^2 + \Pi_0(p)) W_\mu^a W_\nu^a \right. \\ &\quad \left. + \frac{\Pi_1(p)}{4} \frac{h^2}{f^2} \left( W_\mu^1 W_\nu^1 + W_\mu^2 W_\nu^2 + \left( W_\mu^3 - \frac{g'}{g} B_\mu \right) \left( W_\nu^3 - \frac{g'}{g} B_\nu \right) \right) \right],\end{aligned}\quad (3.11)$$



where the transverse and longitudinal projection operators are defined as

$$P_T^{\mu\nu} = g^{\mu\nu} - \frac{p^\mu p^\nu}{p^2}, \quad P_L^{\mu\nu} = \frac{p^\mu p^\nu}{p^2}, \quad (3.12)$$

and the form factor are given by the Weinberg sum rules [40]

$$\Pi_0(p) = \frac{g^2 p^2 f_1^2}{p^2 + m_V^2}, \quad \Pi_1(p) = \frac{g^2 f^2 m_V^2 m_A^2}{(p^2 + m_V^2)(p^2 + m_A^2)}, \quad (3.13)$$

where from the definition of the Fermi decay constant it is obtained that  $f = \sqrt{f_1^2 - r^2 f_2^2}$  [39]. It will be shown in Section 5 that at one-loop level this Lagrangian contributes to the effective Higgs potential.

#### 4 The effective theory of the fermion resonances

In this section, we introduce the effective theory of the fermion resonances, which are important for the generation of the masses and Composite Higgs-Yukawa couplings of the SM fermions. The composite fermion resonances also contribute to the effective Higgs potential in Eq. (5.1) and affect the electroweak precision observables.

We introduce a Dirac **6**-plet of fermionic resonances  $\Psi$  transforming in the antisymmetric representation of  $SU(4)_2$  while the composite spin-1 resonances transform in the adjoint. The fermionic resonances will mix with the elementary doublet  $q_{L,3} = (t_L, b_L)^T$  and the singlet  $t_R$  to provide the top mass. A new  $U(1)_X$  gauge symmetry is introduced to provide the correct hypercharges, embedded in the unbroken  $SO(6)_\chi$  in Eq. (2.2). The SM hypercharge is defined as  $Y = T_{R,1}^3 + T_{R,2}^3 + X$ , where  $T_{R,i}^3$  are the diagonal generators of the subgroups  $SU(2)_{R,i}$  in  $Sp(4)_i$ . The SM  $SU(2)_L$  is the vectorial combination of the  $SU(2)_{L,i}$  subgroups in  $Sp(4)_i$ .

Now, we consider the **1** and **5** representations of the unbroken  $Sp(4)_2$  in  $SU(4)_2$ . Under the decomposition  $Sp(4)_2 \otimes U(1)_X \rightarrow SU(2)_L \otimes U(1)_Y$ , we get the  $SU(2)_L$  singlet  $\Psi_1$  (denoted  $T_1$ ) with  $\mathbf{1}_{2/3}$  and the fiveplet

$$\begin{pmatrix} \mathbf{5}_{2/3} \rightarrow \mathbf{2}_{7/6} \oplus \mathbf{2}_{1/6} \oplus \mathbf{1}_{2/3} \\ \Psi_5 \rightarrow Q_X \oplus Q_5 \oplus T_5 \end{pmatrix}, \quad (4.1)$$

where  $Q_X = (X_{5/3}, X_{2/3})$  and  $Q_5 = (T, B)$ . Their explicit embeddings in representation **6** of  $SU(4)_2$  are [41]

$$\begin{aligned} \Psi_{5L} &= \frac{1}{2} \begin{pmatrix} T_{5L} i\sigma_2 & \sqrt{2} \tilde{Q}_L \\ -\sqrt{2} \tilde{Q}_L^T & T_{5L} i\sigma_2 \end{pmatrix}, & \tilde{Q}_L &= \begin{pmatrix} T_L & X_{5/3,L} \\ B_L & X_{2/3,L} \end{pmatrix}, \\ \Psi_{5R}^c &= \frac{1}{2} \begin{pmatrix} T_{5R}^c i\sigma_2 & \sqrt{2} \tilde{Q}_R^c \\ -\sqrt{2} \tilde{Q}_R^{cT} & T_{5R}^c i\sigma_2 \end{pmatrix}, & \tilde{Q}_R^c &= \begin{pmatrix} -X_{2/3,R}^c & B_R^c \\ X_{5/3,R}^c & -T_R^c \end{pmatrix}, \\ \Psi_{1L} &= \frac{1}{2} \begin{pmatrix} T_{1L} i\sigma_2 & 0 \\ 0 & -T_{1L} i\sigma_2 \end{pmatrix}, & \Psi_{1R}^c &= \frac{1}{2} \begin{pmatrix} T_{1R}^c i\sigma_2 & 0 \\ 0 & -T_{1R}^c i\sigma_2 \end{pmatrix}. \end{aligned} \quad (4.2)$$

In the following, we focus on the case in which both the left- and right-handed top quarks mix with top-partners in the  $\mathbf{6}$  (two-index anti-symmetric) representation of  $SU(4)_2$ , where the wave functions of these top-partners and their quantum number under  $SU(4)_2 \times SU(6)_\chi$  in Eq. (2.2) have the form  $QQ\chi \in (\mathbf{6}, \mathbf{6})$  as in the parentheses in Eq. (2.3). The left-handed fermionic operators of the form  $QQ\chi$  can be decomposed under the unbroken subgroup  $Sp(4)_2 \times SU(3)_C \times U(1)_X$  as

$$\begin{aligned} (\mathbf{6}, \mathbf{6}) &= (\mathbf{5}, \mathbf{3}, 2/3) + (\mathbf{5}, \bar{\mathbf{3}}, -2/3) + (\mathbf{1}, \mathbf{3}, 2/3) + (\mathbf{1}, \bar{\mathbf{3}}, -2/3) \\ &\equiv \Psi_{5L} + \Psi_{5R}^c + \Psi_{1L} + \Psi_{1R}^c, \end{aligned} \quad (4.3)$$

where the explicit matrices of the composite resonances  $\Psi_{5L,5R,1L,1R}$  are given in Eq. (4.2). In order to describe the linear fermion mixing, the top quark doublet and singlet,  $q_L$  and  $t_R$  are embedded as a  $\mathbf{6}$  of  $SU(4)_Q$  as

$$\Psi_{q_L} = \frac{1}{\sqrt{2}} \begin{pmatrix} 0 & Q_{q_L} \\ -Q_{q_L}^T & 0 \end{pmatrix}, \quad Q_{q_L} = \begin{pmatrix} t_L & 0 \\ b_L & 0 \end{pmatrix}, \quad \Psi_{t_R}^c = \frac{t_R^c}{2} \begin{pmatrix} -i\sigma_2 & 0 \\ 0 & i\sigma_2 \end{pmatrix}. \quad (4.4)$$

To leading order, the effective Lagrangian for the elementary and composite fermions can then be decomposed in three parts

$$\mathcal{L}_{\text{ferm}} = \mathcal{L}_{\text{elem}} + \mathcal{L}_{\text{comp}} + \mathcal{L}_{\text{mix}}. \quad (4.5)$$

The Lagrangian for the elementary fermions is

$$\mathcal{L}_{\text{elem}} = i\bar{q}_{L,3}\not{D}q_{L,3} + i\bar{t}_R\not{D}t_R, \quad (4.6)$$

where the covariant derivatives is given by

$$\begin{aligned} D_\mu q_{L,3} &= \left( \partial_\mu - igW_\mu^i \frac{\sigma_i}{2} - i\frac{1}{6}g'B_\mu - ig_S G_\mu \right) q_{L,3}, \\ D_\mu t_L &= \left( \partial_\mu - i\frac{2}{3}g'B_\mu - ig_S G_\mu \right) t_L. \end{aligned} \quad (4.7)$$

The Lagrangian for the composite fermions containing their gauge-kinetic, mass and interaction terms between the fiveplet and singlet can be written as [10, 41]

$$\begin{aligned} \mathcal{L}_{\text{comp}} &= i\text{Tr}[\Psi_{5L}^\dagger \bar{\sigma}^\mu D_\mu \Psi_{5L}] + i\text{Tr}[(\Psi_{5R}^c)^\dagger \sigma^\mu D_\mu \Psi_{5R}^c] \\ &\quad + i\text{Tr}[\Psi_{1L}^\dagger \bar{\sigma}^\mu D_\mu \Psi_{1L}] + i\text{Tr}[(\Psi_{1R}^c)^\dagger \sigma^\mu D_\mu \Psi_{1R}^c] \\ &\quad - (m_5 \text{Tr}[\Psi_{5L} \Sigma_{Q0} \Psi_{5R}^c \Sigma_{Q0}] + m_1 \text{Tr}[\Psi_{1L} \Sigma_{Q0} \Psi_{1R}^c \Sigma_{Q0}] + \text{h.c.}) \\ &\quad - (ic_L \text{Tr}[\Psi_{5L}^\dagger \bar{\sigma}^\mu d_{2,\mu} \Psi_{1L}] + ic_R \text{Tr}[\Psi_{5R}^\dagger \sigma^\mu d_{2,\mu} \Psi_{1R}] + \text{h.c.}), \end{aligned} \quad (4.8)$$

where the covariant derivatives are given by

$$\begin{aligned} D_\mu \Psi_5 &= \left( \partial_\mu - i\frac{2}{3}g'B_\mu T_R^3 - ie_{2,\mu} - ig_S G_\mu \right) \Psi_5, \\ D_\mu \Psi_1 &= \left( \partial_\mu - i\frac{2}{3}g'B_\mu T_R^3 - ig_S G_\mu \right) \Psi_1, \end{aligned} \quad (4.9)$$

and the  $d$  and  $e$  symbols are defined in Eq. (3.4) which contain the heavy spin-1 resonances. Finally, the mixing terms between the SM fermions, composite pNGBs and fermion resonances invariant under  $SU(4)_Q$  are given by [41]

$$\begin{aligned} \mathcal{L}_{\text{mix}} = & -y_{L5}f\text{Tr}[\Psi_{qL}U_Q\Psi_{5R}^cU_Q^T] - y_{L1}f\text{Tr}[\Psi_{qL}U_Q\Psi_{1R}^cU_Q^T] \\ & - y_{R5}f\text{Tr}[\Psi_{tR}^cU_Q\Psi_{5L}U_Q^T] - y_{R1}f\text{Tr}[\Psi_{tR}^cU_Q\Psi_{1L}U_Q^T] + \text{h.c.} . \end{aligned} \quad (4.10)$$

From the effective Lagrangian  $\mathcal{L}_{\text{ferm}}$  in Eq. (4.5), the mass matrix of the top quark and the top-partners with  $+2/3$  charge has the form

$$\begin{pmatrix} \bar{t}_L \\ \bar{T}_{1L} \\ \bar{T}_L \\ \bar{X}_{2/3L} \\ \bar{T}_{5L} \end{pmatrix}^T \begin{pmatrix} 0 & \frac{y_{L1}f}{\sqrt{2}}s_\theta & \frac{y_{L5}f}{2}(1+c_\theta) & \frac{y_{L5}f}{2}(1-c_\theta) & 0 \\ y_{R1}fc_\theta & -m_1 & 0 & 0 & 0 \\ -\frac{y_{R5}f}{\sqrt{2}}s_\theta & 0 & -m_5 & 0 & 0 \\ \frac{y_{R5}f}{\sqrt{2}}s_\theta & 0 & 0 & -m_5 & 0 \\ 0 & 0 & 0 & 0 & -m_5 \end{pmatrix} \begin{pmatrix} t_R \\ T_{1R} \\ T_R \\ X_{2/3R} \\ T_{5R} \end{pmatrix}. \quad (4.11)$$

By diagonalizing this mass matrix, the top mass is easily obtained

$$m_{\text{top}} \simeq \frac{|y_{L1}y_{R1}m_5 - y_{L5}y_{R5}m_1|f}{\sqrt{m_1^2 + y_{R1}^2f^2}\sqrt{m_5^2 + y_{L5}^2f^2}} \frac{v_{\text{EW}}}{\sqrt{2}}, \quad (4.12)$$

while the masses of top-partners with  $+2/3$  charge (in the limit  $c_\theta \sim 1$ ) are given by

$$m_{T_1} \simeq \sqrt{m_1^2 + y_{R1}^2f^2}, \quad m_T \simeq \sqrt{m_5^2 + y_{L5}^2f^2}, \quad m_{X_{2/3}} \simeq m_5, \quad m_{T_5} = m_5. \quad (4.13)$$

For  $m_T \gg m_{T_1}$ , the top mass is approximately given by

$$m_{\text{top}} \simeq \frac{y_{L1}y_{R1}f}{\sqrt{m_1^2 + y_{R1}^2f^2}} \frac{v_{\text{EW}}}{\sqrt{2}} \simeq \frac{y_{L1}y_{R1}f}{m_{T_1}} \frac{v_{\text{EW}}}{\sqrt{2}}. \quad (4.14)$$

Finally, after integrating out the heavy top-partners in Eq. (4.5), we get the effective Lagrangian

$$\begin{aligned} \mathcal{L}_{\text{eff}}^{\text{top}} = & \Pi_0^q(p)\text{Tr}[\bar{\Psi}_{qL}\not{p}\Psi_{qL}] + \Pi_0^t(p)\text{Tr}[\bar{\Psi}_{tR}^c\not{p}\Psi_{tR}^c] \\ & + M_1^t(p)\text{Tr}[\bar{\Psi}_{qL}\Sigma_Q^*\Psi_{tR}^c\Sigma_Q^*] + \text{h.c.}, \end{aligned} \quad (4.15)$$

where the form factors are given by the Weinberg sum rules [40]

$$\begin{aligned} \Pi_0^q(p) &= 1 + \frac{|y_{L5}|^2f^2}{p^2 + m_5^2}, \quad \Pi_0^t(p) = 1 + \frac{|y_{R5}|^2f^2}{p^2 + m_5^2}, \\ M_1^t(p) &= \frac{y_{L1}y_{R1}^*f^2m_1}{p^2 + m_1^2} - \frac{y_{L5}y_{R5}^*f^2m_5}{p^2 + m_5^2}. \end{aligned} \quad (4.16)$$

In the following section, we show that at one-loop level this Lagrangian contributes to the effective Higgs potential.

## 5 The effective potential and vacuum misalignment

The vacuum alignment angle  $\theta$  is controlled by the effective potential  $V_{\text{eff}}$ , which receives contributions from the vector-like masses of the hyper-fermions, the SM fermion couplings to the strong sector and the EW gauge interactions. At leading order, each source of symmetry breaking contributes independently to the effective potential:

$$V_{\text{eff}} = V_{\text{gauge}} + V_{\text{top}} + V_{\text{m}} + \dots, \quad (5.1)$$

where the dots are left to indicate the presence of mixed terms at higher orders, or the effect of additional UV operators.

From the effective Lagrangian in Eq. (3.11), at one-loop level of the gauge interactions we can write the Coleman-Weinberg potential

$$V_{\text{gauge}} = \frac{6}{2} \int \frac{d^4 p}{(2\pi)^4} \log \left( 1 + \frac{\Pi_1}{4\Pi_W} \sin^2 \left( \frac{\pi Q}{f} \right) \right) + \frac{3}{2} \int \frac{d^4 p}{(2\pi)^4} \log \left[ 1 + \left( \frac{g'^2}{g^2} \frac{\Pi_1}{4\Pi_B} + \frac{\Pi_1}{4\Pi_W} \right) \sin^2 \left( \frac{\pi Q}{f} \right) \right], \quad (5.2)$$

where  $\Pi_W = p^2 + \Pi_0$  and  $\Pi_B = p^2 + (g'/g)^2 \Pi_0$ . To leading orders, the Higgs potential from the EW gauge boson loops is

$$V_{\text{gauge}}^0 = \alpha_g s_\theta^2 + \beta_g s_\theta^4 + \mathcal{O}(s_\theta^6), \quad (5.3)$$

where

$$\alpha_g \equiv \frac{3}{8} \int \frac{d^4 p}{(2\pi)^4} \left[ \frac{3}{\Pi_W} + \frac{g'^2}{g^2} \frac{1}{\Pi_B} \right] \Pi_1, \quad (5.4)$$

$$\beta_g \equiv -\frac{3}{64} \int \frac{d^4 p}{(2\pi)^4} \left[ 2 \left( \frac{1}{\Pi_W} \right)^2 + \left( \frac{g'^2}{g^2} \frac{1}{\Pi_B} + \frac{1}{\Pi_W} \right)^2 \right] \Pi_1^2.$$

From the top quark effective Lagrangian in Eq. (4.15), the Higgs potential  $V_{\text{top}}$  at one-loop level in Eq. (5.1) can be computed by using the Coleman-Weinberg formula

$$V_{\text{top}} = -2N_c \int \frac{d^4 p}{(2\pi)^4} \log \left( 1 + \frac{|M_1^t|^2}{2p^2 \Pi_0^q \Pi_0^t} \frac{h^2}{\pi_Q^2} \sin^2 \frac{2\pi Q}{f} \right). \quad (5.5)$$

By expanding  $V_{\text{top}}$  up to  $\mathcal{O}(s_\theta^4)$  and to zero order in the fields, we obtain the effective potential

$$V_{\text{top}}^0 = \alpha_f (-s_\theta^2 + s_\theta^4) + \mathcal{O}(s_\theta^6), \quad (5.6)$$

where

$$\alpha_f \equiv 4N_c \int \frac{d^4 p}{(2\pi)^4} \frac{|M_1^t|^2}{p^2 \Pi_0^q \Pi_0^t}. \quad (5.7)$$

Furthermore, we obtain the potential contributions  $V_{\text{m}}$  in Eq. (5.1) from the hyper-fermion masses given in Eq. (2.1), which is given by

$$V_{\text{m}} = -2\pi Z f^3 \text{Tr}[M_\Psi \Sigma^\dagger] + \text{h.c.} = \gamma_m c_\theta + \dots, \quad (5.8)$$

where we have defined  $\gamma_m \equiv 8\pi Z f^3 m_Q$  and  $m_Q \equiv \bar{m}_1 + \bar{m}_2$ .

To leading order, the effective potential in Eq. (5.1) has the form

$$V_{\text{eff}}^0 = -\alpha s_\theta^2 + \beta s_\theta^4 + \gamma c_\theta + \dots, \quad (5.9)$$

where  $\alpha = \alpha_f - \alpha_g$ ,  $\beta = \alpha_f + \beta_g$  and  $\gamma = \gamma_m$ . For  $\alpha \gg \beta s_\theta^2$ , we obtain the vacuum misalignment angle by minimizing the effective Higgs potential

$$c_\theta \approx -\frac{\gamma}{2\alpha}. \quad (5.10)$$

From the vacuum alignment and the effective potential in Eq. (5.1), the Higgs mass can be expressed as

$$m_h^2 = \frac{2s_\theta^2}{f^2} (\alpha + 2(2 - 3s_\theta^2)\beta). \quad (5.11)$$

## 6 Contributions to the oblique parameters

Now, we are ready to collect the contributions to the oblique parameters from the modification of the Higgs couplings in Eq. (2.10), the composite spin-1 resonances studied in Section 3 and the composite fermion resonances in Section 4.

### 6.1 Modification of the Higgs couplings

The modification of the Higgs couplings to the EW gauge bosons in Eq. (2.10) produces approximately the following deviations in the oblique parameters [39]

$$\begin{aligned} \Delta S &= \frac{1}{6\pi} \left[ (1 - \kappa_V^2) \ln \left( \frac{\Lambda_{\text{HC}}}{m_h} \right) + \ln \left( \frac{m_h}{m_{h,\text{ref}}} \right) \right], \\ \Delta T &= -\frac{3}{8\pi \cos^2 \theta_W} \left[ (1 - \kappa_V^2) \ln \left( \frac{\Lambda_{\text{HC}}}{m_h} \right) + \ln \left( \frac{m_h}{m_{h,\text{ref}}} \right) \right] \end{aligned} \quad (6.1)$$

with the Higgs couplings to the EW gauge bosons normalized to the SM ones

$$\begin{aligned} \kappa_W &= c_\theta + \kappa_{W,\text{res}} \simeq c_\theta + \frac{g^2}{\tilde{g}^2} \frac{1}{2} (1 - r^2) s_\theta^2, \\ \kappa_Z &= c_\theta + \kappa_{Z,\text{res}} \simeq c_\theta + \frac{g^2 + g'^2}{\tilde{g}^2} \frac{1}{2} (1 - r^2) s_\theta^2, \end{aligned} \quad (6.2)$$

where the correction factors  $\kappa_{W/Z,\text{res}}$  from the composite spin-1 resonances are included. For simplicity, we can neglect the term in  $g'^2$  without significant changes, so that  $\kappa_V \sim \kappa_W \sim \kappa_Z$ . Note for a typical coupling  $r \leq 1$  these modifications contribute positively to the  $S$  parameter and negatively to the  $T$  parameter. Therefore, we need a positive contribution to  $T$  from the composite resonances to reproduce the  $S, T$  correlation in the EW precision measurements obtained from the CDF and LEP measurements summarized in Eqs. (1.1) and (1.2).

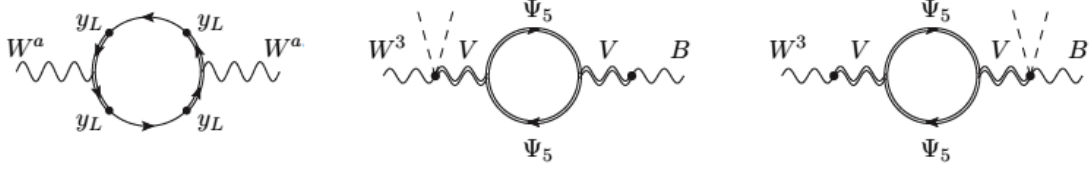


**Figure 1.** Radiative contributions to the  $T$  parameter (left panel diagram) and the  $S$  parameter (middle and right panel diagrams). The straight and wavy double lines represent, respectively, the top-partner spurions and the composite spin-1 resonances.

## 6.2 The composite spin-1 resonances

At leading orders in  $s_\theta$  and  $g/\tilde{g}$  the composite spin-1 contributions to the oblique parameters are given by [39]

$$\begin{aligned}
\Delta\hat{S} &= \frac{g^2(1-r^2)s_\theta^2}{2\tilde{g}^2 + g^2[2 + (r^2 - 1)s_\theta^2]}, \\
\Delta\hat{T} &= 0, \\
\Delta W &= \frac{g^2 m_W^2 [s_\theta^2(r^2 m_V^2 - m_A^2) + 2m_A^2]}{m_A^2 m_V^2 (g^2[(r^2 - 1)s_\theta^2 + 2] + 2\tilde{g}^2)}, \\
\Delta Y &= \frac{g'^2 m_W^2 [s_\theta^2(r^2 m_V^2 - m_A^2) + 2m_A^2]}{m_A^2 m_V^2 (g'^2[(r^2 - 1)s_\theta^2 + 2] + 2\tilde{g}^2)}, \\
\Delta X &= \frac{gg' s_\theta^2 m_W^2 (m_A^2 - r^2 m_V^2)}{m_A^2 m_V^2 \sqrt{(g^2[(r^2 - 1)s_\theta^2 + 2] + 2\tilde{g}^2)(g'^2[(r^2 - 1)s_\theta^2 + 2] + 2\tilde{g}^2)}}.
\end{aligned} \tag{6.3}$$

In our analysis, we are going to use the notation adopted by the PDG and rescale

$$\frac{\alpha_Z S}{4s_W^2} = \Delta\hat{S} - \Delta Y - \Delta W, \quad \alpha_Z T = \Delta\hat{T} - \frac{s_W^2}{1 - s_W^2} \Delta Y, \tag{6.4}$$

where the Weinberg angle  $s_W \equiv \sin \theta_W \simeq 0.223$  and the fine-structure constant at the  $Z$  boson mass  $\alpha_Z \equiv \alpha(m_Z) \simeq 1/127.916$ . Again these resonances contribute positively to  $S$  and a negligible (negative)  $T$ . Therefore, the positive  $T$  contribution must come from the fermion resonances.

## 6.3 The fermion resonances

We calculate the contribution from the fermion resonances in three different scenarios, where we include the contributions from

- (i) only a light top-partner singlet,  $T_1$ ,
- (ii) only a light top-partner from the fiveplet,  $T$ , and
- (iii) both the singlet and fiveplet.

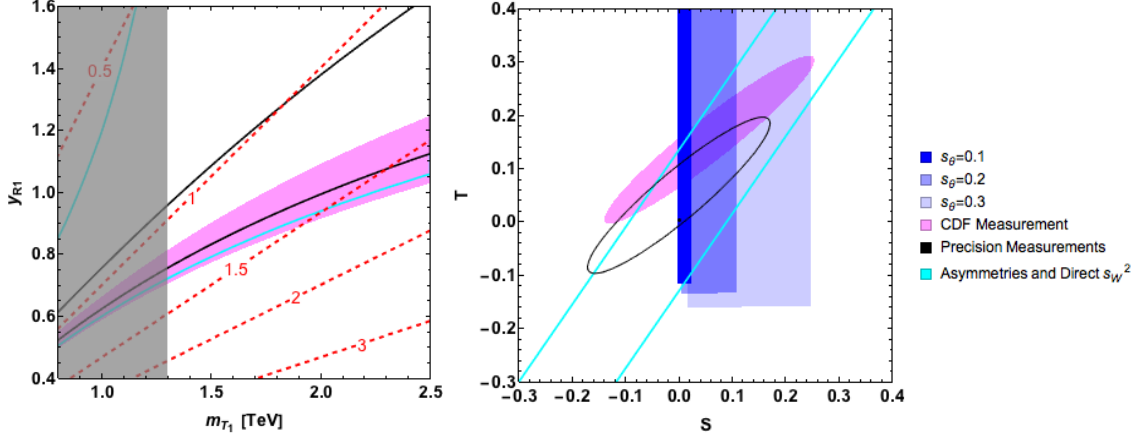


**Figure 2.** Comparison of the new CDF measurement of the W mass (magenta band) to the parameter space of the  $SU(4)_Q/Sp(4)_Q$  Composite Higgs model, including only the  $S$  and  $T$  contributions from the fermion resonance singlet. Between the black lines or in the ellipse the precision measurements are fulfilled, while the cyan lines indicate the bound stemming from asymmetries and direct  $s_W^2$  determination. All bounds are shown at  $2\sigma$  confidence level. *Left panel:* The bands in the  $m_{T_1}$ - $y_{R1}$  parameter space for  $s_\theta = 0.2$ ,  $m_{V,A} = 3$  TeV,  $\tilde{g} = 3$  and  $r = 0.8$ , where the dashed red lines represent the values of  $y_{L1}$ . The gray region is excluded by the lower bound on  $m_{T_1} \gtrsim 1.3$  TeV from CMS and ATLAS [43–46]. *Right panel:* The bands in the  $S$ - $T$  parameter space, where the blue regions represent the parameter space of the model for  $s_\theta = 0.1, 0.2, 0.3$ . We have scanned over  $\tilde{g} \geq 3$ ,  $0.5 \leq y_{R1} \leq 5$ ,  $m_{V,A} \geq 3$  TeV and  $0 \leq r \leq 1$ , while  $m_{T_1} \geq 1.3$  TeV from CMS and ATLAS [43–46].

**Scenario (i):** In this case in which only the top-partner singlet,  $T_1$ , is light, the  $T$  parameter receives a sizable positive contribution from loops of the fermion resonances as the diagram in the left-handed panel of Figure 1, while the contribution to the  $S$  parameter of the two other diagrams to the right is negligible. At leading order in  $s_\theta$ , the explicit results read

$$\begin{aligned} \Delta\hat{S} &\simeq 0, \\ \Delta\hat{T} &= \frac{3}{64\pi^2} \frac{y_{L1}^4 m_1^4 v_{\text{SM}}^2}{(m_1^2 + y_{R1}^2 f^2)^3} \left[ 1 + \frac{2y_{R1}^2 f^2}{m_1^2} \left( \log \left( \frac{2(m_1^2 + y_{R1}^2 f^2)^2}{y_{L1}^2 y_{R1}^2 f^4 s_\theta^2} \right) - 1 \right) \right]. \end{aligned} \quad (6.5)$$

In a large part of the parameter space, this contribution can compensate the negative  $T$  contribution from the modification of the Higgs couplings in Eq. (6.1) and reproduce the  $S, T$  correlations found in fits to observations.

In the present model example, we have nine free parameters  $y_{L1,R1}$ ,  $m_1$ ,  $m_{V,A}$ ,  $\tilde{g}$ ,  $r$ ,  $f$  and  $s_\theta$  in the above expressions of the  $S$  and  $T$  parameters. In the following, we fix the parameters of the composite spin-1 resonances  $m_{V,A} = 3$  TeV,  $\tilde{g} = 3$  and  $r = 0.8$ . Changes in these parameters have small effects on the following conclusions. Furthermore, we can determine  $y_{L1}$  by fixing the top mass for  $m_T \gg m_{T_1}$  in Eq. (4.14), determine  $f$  by fixing the EW VEV in Eq. (2.11) and replace  $m_1$  with the lightest top-partner mass  $m_{T_1}$  in Eq. (4.13). This reduces the number of free parameters to three:  $y_{R1}$ ,  $m_{T_1}$  and the vacuum alignment angle  $s_\theta$ .

In Figure 2, the parameter space of the minimal CH model with only the fermion resonance singlet is shown which is constrained by the new CDF measurement in Eq. (1.1), depicted by the magenta band or ellipse. Between the black lines or inside the black ellipse the precision measurements in Eq. (1.2) are satisfied, while the cyan lines indicate the bound stemming from asymmetries and direct  $s_W^2$  determination in the SM [42]. All bounds are shown at  $(2\sigma)$  95% confidence level. In the left-handed panel, the bands are shown in the  $m_{T_1}$ - $y_{R1}$  parameter space with  $s_\theta = 0.2$ , where the dashed red lines represent the values of  $y_{L1}$ . The lower bound on  $m_{T_1} \gtrsim 1.3$  TeV is given by CMS and ATLAS [43–46], which excludes the gray region. There is thus a viable area in the parameter space with  $y_{L1,R1}$  of order unity that satisfies the new CDF and/or LEP measurements along with the lower bounds on  $m_{T_1}$  and from the asymmetries and direct  $s_W^2$  determination. In the right-handed panel, the bands are shown in the  $S$ - $T$  parameter space, where the blue regions represent the parameter space of the model for  $s_\theta = 0.1, 0.2, 0.3$ . We have scanned over  $\tilde{g} \geq 3$ ,  $0.5 \leq y_{R1} \leq 5$ ,  $m_{V,A} \geq 3$  TeV and  $0 \leq r \leq 1$ , while  $m_{T_1} \geq 1.3$  TeV from CMS and ATLAS [43–46]. Thus, there are viable regions in the parameter space for  $s_\theta \leq 0.3$ . Therefore, the constraints on  $s_\theta$  from the EW precision measurements (also the recent CDF results) are weaker than the bound from the Higgs couplings to the EW gauge bosons in Eq. (2.10), setting the constraint  $s_\theta \lesssim 0.3$  [38].

**Scenario (ii):** Now only a light top-partner,  $T$ , from the fiveplet of the fermion resonance spectrum is included. In this case, the dominant  $S$  contribution (the two diagrams to the right in Figure 1) comes from loops of fermion resonances, where the lightest vector resonances mix with the EW gauge bosons in Eq. (3.8). This contribution is given by the logarithmical corrections

$$\Delta\hat{S} = \frac{g^2 s_\theta^2}{8\pi^2} (1 - c_L^2 - c_R^2) \log\left(\frac{m_V^2}{m_5^2}\right). \quad (6.6)$$

From now on, we choose  $c_L = c_R = 0$  in Eq. (4.8) by assuming that these interactions are weak. Moreover, the  $T$  contribution from the diagram in the left panel in Figure 1 with the fiveplet top-partner,  $T$ , running in the loop is given by

$$\Delta\hat{T} = -\frac{y_{L5}^4}{32\pi^2} \left(\frac{v_{\text{SM}}}{m_5}\right)^2, \quad (6.7)$$

which is always negative. Thus, this scenario has difficulty satisfying the EW precision measurements.

**Scenario (iii):** In the last scenario, we include the contributions from both the singlet and fiveplet, where all the  $S$  and  $T$  contributions in Eqs. (6.1)-(6.7) must be included in the following calculations. Therefore, the positive  $T$  contribution from the top-partner singlet in Eq. (6.5) has to compensate the negative contributions from the modification of the Higgs couplings in Eq. (6.1) and the fiveplet in Eq. (6.7).

As in the case (i), we fix  $m_{V,A} = 3$  TeV,  $\tilde{g} = 3$  and  $r = 0.8$  due to the fact that changes of them have small effects on the following results. We assume  $y_{L1} = y_{L5} \equiv y_L$  and



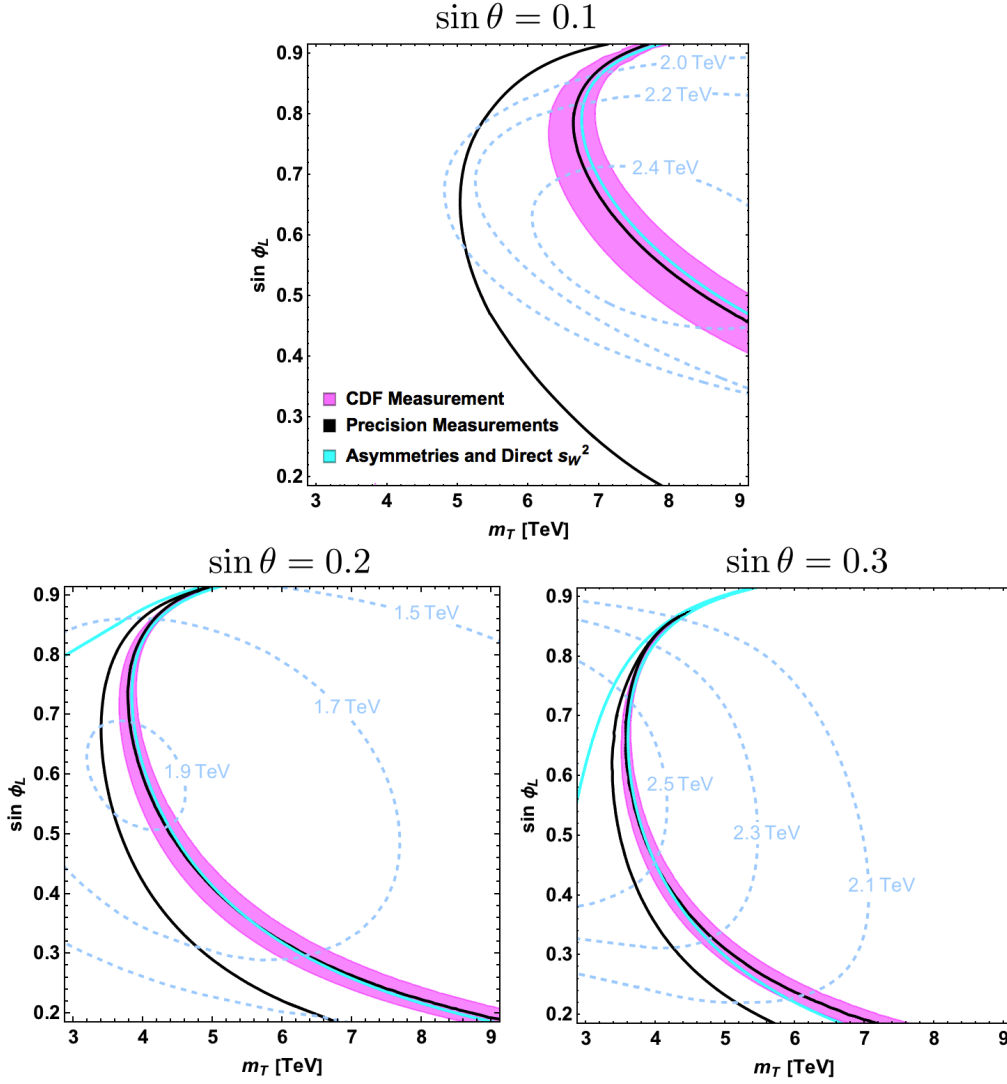


**Figure 3.** Comparison of the new CDF measurement of the W mass (magenta band) to the  $m_T$ - $\sin \phi_L$  parameter space of the minimal CH model for  $s_\theta = 0.1, 0.2, 0.3$ , including the  $S$  and  $T$  contributions from both the fermion resonance singlet and fiveplet. Between the black lines the precision measurements are fulfilled, while the cyan lines indicate the bound stemming from asymmetries and direct  $s_W^2$  determination. All bounds are shown at  $2\sigma$  confidence level and for  $m_{V,A} = 3$  TeV,  $\tilde{g} = 3$  and  $r = 0.8$ . The dashed lines represent the top-partner singlet mass,  $m_{T_1}$ .

$y_{R1} = y_{R5} \equiv y_R$ , while we use the expressions of the EW VEV in Eq. (2.11), the top mass in Eq. (4.12), the masses of the two lightest fermion resonances  $T_1$  and  $T$  in Eq. (4.13) and the Higgs mass in Eq. (5.11). These expressions reduce the number of free parameters from ten  $y_{L1,R1,L5,R5}$ ,  $m_{T_1,T}$ ,  $m_{1,5}$ ,  $f$  and  $s_\theta$  to three  $m_T$ ,  $s_{\phi_L}$  and  $s_\theta$ , where we have defined the  $q_L$  compositeness angle given by

$$\sin \phi_L \equiv \frac{y_L f}{\sqrt{m_5^2 + y_L^2 f^2}}. \quad (6.8)$$

In Figure 3, the  $m_T$ - $s_{\phi_L}$  parameter space is shown for the minimal CH model with both the fermion resonance singlet and fiveplet, which is constrained by the new CDF measurement of the W mass, depicted by the magenta band. The same bands as in Figure 2 are depicted and all at  $(2\sigma)$  95% confidence level. In this figure, we consider these bands for  $s_\theta = 0.1, 0.2, 0.3$ . The dashed lines represent the values of the top-partner singlet mass,  $m_{T_1}$ . As in scenario (i), the bound on  $s_\theta$  from the Higgs couplings to the EW gauge bosons in Eq. (2.10), setting the constraint  $s_\theta \lesssim 0.3$  [38], is stronger than the constraints from both the recent CDF and the LEP precision measurements. Furthermore, the lower bound on the lightest top-partner (the singlet)  $m_{T_1} \gtrsim 1.3$  TeV from CMS and ATLAS [43–46] does not narrow the parameter space shown in Figure 3 for these values of  $s_\theta$ , only for large  $m_T$  as in case (i). For small  $s_{\phi_L}$ , this lower bound on  $m_{T_1}$  leads to the constraint  $m_T \lesssim 77$  TeV ( $s_{\phi_L} \gtrsim 0.019$ ) for  $s_\theta = 0.2$  and no constraints for  $s_\theta = 0.1$  and  $0.3$ . However, for  $s_\theta = 0.3$ , there is the upper bound  $m_T \lesssim 26$  TeV from the condition  $s_{\phi_L} > 0$ . Finally, we will not consider the bounds in the case with large  $s_{\phi_L}$  due to the fact that the bands depicted in the figure are very narrow in these regions and therefore very fine-tuned in  $s_{\phi_L}$ .

## 7 Generalization to other 4D CH models

The EW precision tests of the minimal CH model studied in this paper can be generalized to non-minimal models. In general, CH model arising from an underlying four-dimensional gauge theory, contain at least one HC representation  $\mathcal{R}$  with  $N_f$  Weyl hyper-fermions, providing a SM-like composite pNGB Higgs multiplet with custodial symmetry after the condensation. Depending on this representation, there exist three possible types of vacuum cosets [34]:  $SU(N_f)/SO(N_f)$  for real  $\mathcal{R}$ ,  $SU(N_f)/Sp(N_f)$  for pseudo-real  $\mathcal{R}$  and  $SU(N_f) \otimes SU(N_f)/SU(N_f) \otimes U(1)$  for complex  $\mathcal{R}$ . For these three types, the minimal CH cosets contain  $N = 5$  in the real case [2],  $N = 4$  in both the pseudo-real [19] and the complex cases [23]. In terms of pNGB spectrum, the pseudo-real case considered in this paper has the fewest number of pNGB states with only five.

For all those CH models, the Higgs couplings to the EW gauge bosons are generally modified by  $c_\theta$  as in Eq. (6.2), providing the  $S$  and  $T$  contributions in Eq. (6.1). The contributions from the spin-1 resonances in Eq. (6.3) are in general determined by the lightest vector and axial-vector  $SU(2)_V$  triplets so also this contribution will only vary slightly between models as long as the underlying fermion dynamics is not vastly different (e.g. QCD-like versus near-conformal). In all cases, variations will have a modest impact due to the smallness of the  $S$  parameter and especially  $T$  parameter contributions. Finally, the top-partner singlet, similar to the singlet  $T_1$ , are also present in the non-minimal CH models, where either the left- or right-handed top quarks are transforming as two-index anti-symmetric under the unbroken chiral symmetry group for both the coset  $SU(N_f)/Sp(N_f)$  and  $SU(N_f) \otimes SU(N_f)/SU(N_f) \otimes U(1)$  or transforming two-index symmetric for the coset  $SU(N_f)/SO(N_f)$  (model examples of these kinds are considered in Ref. [47] with the minimal cosets  $SU(5)/SO(5)$ ,  $SU(4)/Sp(4)$  and  $SU(4)^2 \otimes U(1)/SU(4) \otimes U(1)$ ). The presence of the  $T_1$  type singlets will contribute positively to the  $T$  parameter and provided this is the lightest fermion resonance this contribution will dominate leading to the  $S, T$  parameter

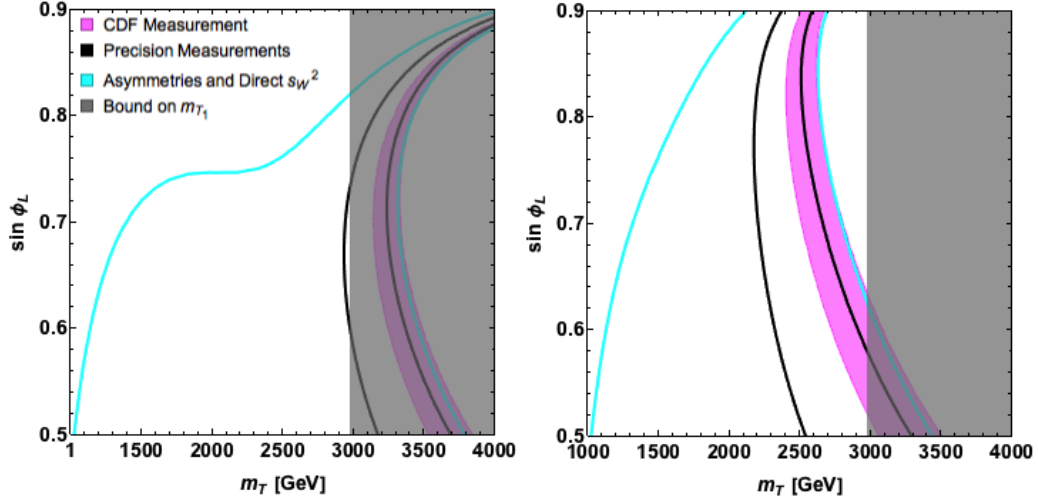


**Figure 4.** Comparison of the new CDF measurement of the  $W$  mass (magenta band) to the  $m_T$ - $\sin\phi_L$  parameter space of the  $SO(5)/SO(4)$  CH model for  $s_\theta = 0.2$ , including the  $S$  and  $T$  contributions from both the fermion resonance singlet and fourplet. Between the black lines the precision measurements are fulfilled, while the cyan lines indicate the bound stemming from asymmetries and direct  $s_W^2$  determination. All bounds are shown at  $2\sigma$  confidence level and for  $m_{V,A} = 3$  TeV,  $\tilde{g} = 3$  and  $r = 0.8$ . The coupling  $y_R$  is determined up to a twofold ambiguity, where the bands in the  $m_T$ - $\sin\phi_L$  parameter space are shown for the smallest (largest)  $y_R$  solution in the left (right) panel. The gray regions are excluded by the lower bound on  $m_{T_1} \gtrsim 1.3$  TeV from CMS and ATLAS [43–46].

correlation and offset observed in current precision electroweak measurements and underscored by the recent CDF  $W$ -mass measurement. On the other hand, the higher dimensional multiplets, for example the fiveplet considered in this paper, may contribute with negative  $S$  and  $T$  contributions with similar form as given by Eqs. (6.6) and (6.7), respectively, which can be suppressed by their masses. Furthermore, we can not completely exclude the possibility that those multiplets can contribute positively to the oblique parameters.

We leave a detailed study of the contributions from those multiplets for future work. Nevertheless, it is likely that we can draw similar conclusions for these non-minimal models as in the case of the minimal model example.

## 8 CH models with coset $SO(N_f)/SO(N_f - 1)$

Notice that the top-partner resonance  $T_5$  in the fiveplet in Eq. (4.1) does not contribute to the oblique parameters due to the fact that it does not mix with the top quark in the mass matrix in Eq. (4.11). In a CH model with coset  $SO(5)/SO(4)$ , proposed in Ref. [20], the fiveplet is replaced by a fourplet without the top-partner  $T_5$  and, therefore, the results in this paper will also be valid for this CH model. However, this model is difficult to realize in a 4D theory. For example, such a setup may require a 5D theory, described by the holographic approach [20]. Generally, in models with cosets  $SO(N_f)/SO(N_f - 1)$  (e.g.  $SO(5)/SO(4)$ ), the explicit masses of the hyper-fermions in Eq. (2.1) can not be included,

leading to a modification of the Higgs mass in Eq. (5.11):

$$m_h^2 = \frac{8\beta}{f^2} s_\theta^2 c_\theta^2, \quad (8.1)$$

where  $s_\theta^2 = \alpha/(2\beta)$  by minimizing the Higgs potential in Eq. (5.9) with  $\gamma_m = 0$ . In Ref. [10], a relation between the masses of the Higgs boson, the top quark and the top partners is derived:

$$\frac{m_h^2}{m_t^2} \simeq \frac{2N_c}{\pi^2} \frac{m_{T_1}^2 m_T^2 \log(m_T/m_{T_1})}{f^2 (m_T^2 - m_{T_1}^2)}, \quad (8.2)$$

which relates the masses of the singlet and fourplet top-partners,  $m_{T_1}$  and  $m_T$ , by fixing the Higgs and top mass. By repeating the calculations of the oblique parameters from the modification of the Higgs couplings and the spin-1 resonances, we obtain similar expressions of them as in Eqs. (6.1) and (6.3), respectively.

In the following, we choose  $y_{L1} = y_{L5} \equiv y_L$  and  $y_{R1} = y_{R5} \equiv y_R$  for simplicity. For  $s_\theta = 0.2$ ,  $m_{V,A} = 3$  TeV,  $\tilde{g} = 3$  and  $r = 0.8$ , the  $m_T$ - $\sin \phi_L$  parameter space is shown in Figure 4 for the CH model with coset  $\text{SO}(5)/\text{SO}(4)$ , where both the fermion resonance singlet and fourplet are included. This parameter space is constrained by the same bands as in Figure 3, while the gray regions are excluded by the lower bound on  $m_{T_1} \gtrsim 1.3$  TeV from CMS and ATLAS [43–46]. The coupling  $y_R$  is determined up to a twofold ambiguity, where the bands are shown for the smallest and largest  $y_R$  solution in the left and right panel in the figure, respectively. This analysis can also be generalized to  $\text{SO}(N_f)/\text{SO}(N_f - 1)$  by following the same arguments as presented in the previous section. In the case where either the left- or right-handed top quarks are transforming two-index antisymmetric under the unbroken  $\text{SO}(N_f - 1)$ , there will always be a singlet top-partner,  $T_1$ , contributing positively to the  $T$  parameter. Moreover, the same top-partner,  $T$ , of the fourplet will always be present in one of the larger multiplets. By assuming that the additional top-partners are heavier than  $T_1$  and  $T$ , the conclusions from the analysis of the cosets  $\text{SO}(N_f)/\text{SO}(N_f - 1)$  will be almost unchanged compared to the above analysis of the minimal  $\text{SO}(5)/\text{SO}(4)$  coset.

## 9 Conclusions

In this paper, we have computed the oblique electroweak  $S$  and  $T$  parameters in a minimal Composite Higgs model arising from an underlying 4D strongly interacting fermion-gauge theory. The CH sector consists of four Weyl fermions in a pseudo-real representation of a new strongly interacting gauge group and the SM fermion masses arise from linear mixings of interaction eigenstate SM fermions with composite fermions arising from additional strongly interacting fermions of the model. The obtained results generalize to other non-minimal CH models arising from an underlying 4D gauge-fermion theory with fermion partial compositeness.

The Composite Higgs sector leads to a small and positive electroweak  $S$  parameter of  $O(1/6\pi)$  along with a negative  $T$  parameter of similar size. The dominant source for these are the coposite Higgs couplings to SM gauge bosons which are reduced with respect to

the SM Higgs. The contributions from spin-1 resonances are smaller still, so the Composite Higgs sector in isolation is not in agreement with the best fit  $S$  and  $T$  parameter values which favor a positive correlation between  $S$  and  $T$ . However, the fermion partial compositeness sector leads to a positive  $T$  parameter in a large part of parameter space for which we find good agreement between the model and current electroweak precision measurement of the  $S$  and  $T$  parameters, even including the recent CDF  $W$ -boson mass measurement, including the offset and correlation of  $S, T$  with respect to the SM predictions. This requires light composite fermions around the TeV scale, but in agreement with current LHC direct search limits from ATLAS and CMS. If the 2022 CDF results are interpreted in terms of Composite Higgs models, they may offer a striking first window into origin of the SM fermion masses. It will be interesting to further explore the implications for other possible fermion mass origins, in particular “Extended Technicolor” (ETC) [21] and partially composite Higgs models [48], as well as the complementarity of precision electroweak measurements with other probes of the SM fermion mass origin [22].

## Acknowledgements

MTF and MR acknowledge partial funding from The Independent Research Fund Denmark, grant numbers DFF 6108-00623 and DFF 1056-00027B, respectively. We would also like to thank Giacomo Cacciapaglia for useful discussions.

## References

- [1] D. B. Kaplan and H. Georgi, “SU(2) x U(1) Breaking by Vacuum Misalignment,” *Phys. Lett.* **136B** (1984) 183–186.
- [2] M. J. Dugan, H. Georgi and D. B. Kaplan, “Anatomy of a Composite Higgs Model,” *Nucl. Phys.* **B254** (1985) 299–326.
- [3] H. Terazawa, K. Akama and Y. Chikashige, “Unified Model of the Nambu-Jona-Lasinio Type for All Elementary Particle Forces,” *Phys. Rev. D* **15** (1977), 480.
- [4] H. Terazawa, “Subquark Model of Leptons and Quarks,” *Phys. Rev. D* **22** (1980), 184.
- [5] D. B. Kaplan, “Flavor at SSC energies: A New mechanism for dynamically generated fermion masses,” *Nucl. Phys. B* **365** (1991), 259-278.
- [6] G. Cacciapaglia, C. Pica and F. Sannino, “Fundamental Composite Dynamics: A Review,” *Phys. Rept.* **877** (2020), 1-70, [2002.04914].
- [7] M. E. Peskin and T. Takeuchi, “Estimation of oblique electroweak corrections,” *Phys. Rev. D* **46** (1992), 381-409.
- [8] R. Barbieri, A. Pomarol, R. Rattazzi and A. Strumia, “Electroweak symmetry breaking after LEP-1 and LEP-2,” *Nucl. Phys. B* **703** (2004), 127-146, [0405040].
- [9] C. Grojean, O. Matsedonskyi and G. Panico, “Light top partners and precision physics,” *JHEP* **10** (2013), 160, [1306.4655].
- [10] G. Panico and A. Wulzer, “The Composite Nambu-Goldstone Higgs,” *Lect. Notes Phys.* **913** (2016), pp.1-316, [1506.01961].

- [11] S. Schael *et al.* [ALEPH, DELPHI, L3, OPAL and LEP Electroweak], “Electroweak Measurements in Electron-Positron Collisions at W-Boson-Pair Energies at LEP,” *Phys. Rept.* **532** (2013), 119-244, [[1302.3415](#)].
- [12] T. Aaltonen *et al.* [CDF], “High-precision measurement of the W boson mass with the CDF II detector,” *Science* **376** (2022) no.6589, 170-176.
- [13] M. Aaboud *et al.* [ATLAS], “Measurement of the W-boson mass in pp collisions at  $\sqrt{s} = 7$  TeV with the ATLAS detector,” *Eur. Phys. J. C* **78** (2018) no.2, 110 [erratum: *Eur. Phys. J. C* **78** (2018) no.11, 898], [[1701.07240](#)].
- [14] P. A. Zyla *et al.* [Particle Data Group], “Review of Particle Physics,” *PTEP* **2020** (2020) no.8, 083C01.
- [15] [ALEPH, CDF, D0, DELPHI, L3, OPAL, SLD, LEP Electroweak Working Group, Tevatron Electroweak Working Group, SLD Electroweak and Heavy Flavour Groups], “Precision Electroweak Measurements and Constraints on the Standard Model,” [[1012.2367](#)].
- [16] A. Strumia, “Interpreting electroweak precision data including the W-mass CDF anomaly,” [[2204.04191](#)].
- [17] C. T. Lu, L. Wu, Y. Wu and B. Zhu, “Electroweak Precision Fit and New Physics in light of W Boson Mass,” [[2204.03796](#)].
- [18] G. Cacciapaglia and F. Sannino, “The W boson mass weighs in on the non-standard Higgs,” *Phys. Lett. B* **832** (2022), 137232, [[2204.04514](#)].
- [19] J. Galloway, J. A. Evans, M. A. Luty and R. A. Tacchi, “Minimal Conformal Technicolor and Precision Electroweak Tests,” *JHEP* **10** (2010) 086, [[1001.1361](#)].
- [20] K. Agashe, R. Contino and A. Pomarol, “The Minimal composite Higgs model,” *Nucl. Phys. B* **719** (2005), 165-187, [[0412089](#)].
- [21] S. Dimopoulos and L. Susskind, “Mass Without Scalars,” *Nucl. Phys. B* **155** (1979) 237–252.
- [22] T. Alanne, M. T. Frandsen and D. Buarque Franzosi, “Testing a dynamical origin of Standard Model fermion masses,” *Phys. Rev. D* **94**, 071703 (2016), [[1607.01440](#)].
- [23] T. Ma and G. Cacciapaglia, “Fundamental Composite 2HDM: SU(N) with 4 flavours,” *JHEP* **03** (2016), 211, [[1508.07014](#)].
- [24] Y. Wu, T. Ma, B. Zhang and G. Cacciapaglia, “Composite Dark Matter and Higgs,” *JHEP* **11** (2017), 058, [[1703.06903](#)].
- [25] C. Cai, G. Cacciapaglia and H. H. Zhang, “Vacuum alignment in a composite 2HDM,” *JHEP* **01** (2019), 130, [[1805.07619](#)].
- [26] T. Alanne, D. Buarque Franzosi, M. T. Frandsen and M. Rosenlyst, “Dark matter in (partially) composite Higgs models,” *JHEP* **12** (2018), 088, [[1808.07515](#)].
- [27] G. Cacciapaglia, H. Cai, A. Deandrea and A. Kushwaha, “Composite Higgs and Dark Matter Model in SU(6)/SO(6),” *JHEP* **10** (2019), 035, [[1904.09301](#)].
- [28] C. Cai, H. H. Zhang, G. Cacciapaglia, M. Rosenlyst and M. T. Frandsen, “Higgs Boson Emerging from the Dark,” *Phys. Rev. Lett.* **125** (2020) no.2, 021801, [[1911.12130](#)].
- [29] C. Cai, H. H. Zhang, M. T. Frandsen, M. Rosenlyst and G. Cacciapaglia, “XENON1T solar axion and the Higgs boson emerging from the dark,” *Phys. Rev. D* **102** (2020) no.7, 075018, [[2006.16267](#)].

- [30] G. Cacciapaglia, M. T. Frandsen, W. C. Huang, M. Rosenlyst and P. Sørensen, “Techni-Composite Higgs models with (a)symmetric dark matter candidates,” [[2111.09319](#)].
- [31] M. Rosenlyst, “Composite self-interacting dark matter and Higgs,” [[2112.14759](#)].
- [32] E. Witten, “Current Algebra, Baryons, and Quark Confinement,” *Nucl. Phys.* **B223** (1983) 433–444.
- [33] D. A. Kosower, “Symmetry breaking patterns in pseudoreal and real gauge theories,” *Phys. Lett.* **144B** (1984) 215–216.
- [34] M. E. Peskin, “The Alignment of the Vacuum in Theories of Technicolor,” *Nucl. Phys. B* **175** (1980), 197-233.
- [35] J. Barnard, T. Gherghetta and T. S. Ray, “UV descriptions of composite Higgs models without elementary scalars,” *JHEP* **02** (2014), 002, [[1311.6562](#)].
- [36] G. Ferretti and D. Karateev, “Fermionic UV completions of Composite Higgs models,” *JHEP* **03** (2014), 077, [[1312.5330](#)].
- [37] T. Alanne, N. Bizot, G. Cacciapaglia and F. Sannino, “Classification of NLO operators for composite Higgs models,” *Phys. Rev. D* **97** (2018) no.7, 075028, [[1801.05444](#)].
- [38] J. de Blas, O. Eberhardt and C. Krause, “Current and Future Constraints on Higgs Couplings in the Nonlinear Effective Theory,” *JHEP* **07** (2018) 048, [[1803.00939](#)].
- [39] D. Buarque Franzosi, G. Cacciapaglia, H. Cai, A. Deandrea and M. Frandsen, “Vector and Axial-vector resonances in composite models of the Higgs boson,” *JHEP* **11** (2016), 076, [[1605.01363](#)].
- [40] L. Bian, Y. Wu and K. P. Xie, “Electroweak phase transition with composite Higgs models: calculability, gravitational waves and collider searches,” *JHEP* **12** (2019), 028, [[1909.02014](#)].
- [41] Z. Y. Dong, C. S. Guan, T. Ma, J. Shu and X. Xue, “UV completed composite Higgs model with heavy composite partners,” *Phys. Rev. D* **104** (2021) no.3, 035013, [[2011.09460](#)].
- [42] J. Haller, A. Hoecker, R. Kogler, K. Mönig, T. Peiffer and J. Stelzer, “Update of the global electroweak fit and constraints on two-Higgs-doublet models,” *Eur. Phys. J. C* **78** (2018) no.8, 675, [[1803.01853](#)].
- [43] M. Aaboud *et al.* [ATLAS], “Combination of the searches for pair-produced vector-like partners of the third-generation quarks at  $\sqrt{s} = 13$  TeV with the ATLAS detector,” *Phys. Rev. Lett.* **121** (2018) no.21, 211801, [[1808.02343](#)].
- [44] A. M. Sirunyan *et al.* [CMS], “Search for vector-like T and B quark pairs in final states with leptons at  $\sqrt{s} = 13$  TeV,” *JHEP* **08** (2018), 177, [[1805.04758](#)].
- [45] A. M. Sirunyan *et al.* [CMS], “Search for pair production of vector-like quarks in the  $bW\bar{b}W$  channel from proton-proton collisions at  $\sqrt{s} = 13$  TeV,” *Phys. Lett. B* **779** (2018), 82-106, [[1710.01539](#)].
- [46] A. M. Sirunyan *et al.* [CMS], “Search for pair production of vectorlike quarks in the fully hadronic final state,” *Phys. Rev. D* **100** (2019) no.7, 072001, [[1906.11903](#)].
- [47] G. Ferretti, “Gauge theories of Partial Compositeness: Scenarios for Run-II of the LHC,” *JHEP* **06** (2016), 107, [[1604.06467](#)].
- [48] T. Alanne, D. Buarque Franzosi and M. T. Frandsen, “A partially composite Goldstone Higgs,” *Phys. Rev. D* **96**, no.9, 095012 (2017), [[1709.10473](#)].